ACS APPLIED MATERIALS & INTERFACES

Research Article

www.acsami.org

Statistical Analysis of Plating Variable Effects on the Electrical Conductivity of Electroless Copper Patterns on Paper

Daniel Zabetakis and Walter J. Dressick*

U.S. Naval Research Laboratory, Center for Bio/Molecular Science & Engineering, Code 6910, 4555 Overlook Avenue S.W., Washington, D.C. 20375, United States

Supporting Information

ABSTRACT: We describe a process for selective metallization of paper substrates bearing inkjet printed patterns of a commercial Pd/Sn colloidal catalyst ink plated using a commercial electroless Cu bath. The electrical conductivity of the Cu films is analyzed as a function of feature geometry (line dimensions (L) and spacing (S)), type of paper (P), age of the Pd/Sn patterns (A), plating time (T), and plating temperature (H) using a two-level factorial design. Conductivity is influenced predominantly by the P, T, and H factors, with lesser contributions attributed to pair-wise interactions among several of the variables studied. Increases in T and/or H enhance conductivity of the Cu films, whereas increases in P, corresponding to the use of rougher, more porous, paper substrates, yield Cu films exhibiting decreased conductivity. Our analysis leads to a model that predicts Cu film conductivity well over the ranges of variables examined, provides guidelines for identification of optimum conditions for plating highly conductive Cu films, and identifies areas for further process improvement.

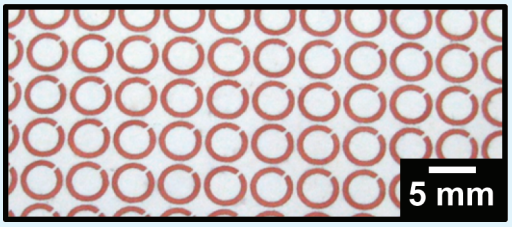

KEYWORDS: *inkjet printing, pattern, electroless, factorial analysis, paper, cellulose*

INTRODUCTION

The ability to fabricate patterned metal features useful as electrical interconnects,[1−4] antennae,[5,6] or RF shields[7,8] on flexible polymer thin films is becoming increasingly important for applications requiring the integration of electronic components into non-conventional and non-planar substrates such as natural or synthetic textiles. Given the lower-resolution features (i.e., mils) often comprising such metal structures, inkjet printing (IJP) is attracting significant attention as a direct-write process for mass production.[9−18] This interest in IJP is due, at least in part, to its potential for high throughput (e.g., reel-to-reel production) manufacture, process flexibility, simplicity, and low cost.[19]

IJP patterning processes associated with fabrication of metallic features typically involve deposition of an ink containing metallic nanoparticles dispersed in a suitably volatile solvent onto the polymer substrate.[10,12,18] This step is followed by thermal annealing to fix the pattern via solvent evaporation and nanoparticle sintering, which provides the direct nanoparticle connectivity required for electrical conductivity.[6,10,12,13,17,20] Au, Ag, and Cu nanoparticles exhibit sufficient electrical conductivity for use as inks, with Cu preferred because of its reasonable cost. However, the ease of oxidation of Cu can present problems regarding ink dispersion stability and sintering efficiency.[21−23]

In addition, substrates are limited to those polymers capable of withstanding the sintering process without thermal decomposition or alteration of their desirable physicochemical properties. Although good progress in lowering sintering temperatures continues to be made,[20,24,25] this requirement often precludes the use of many biopolymers despite their otherwise attractive properties. For example, as the most abundant biopolymer, cellulose has long served as a renewable raw material sustaining the textile and papermaking industries, among others.[26,27] As a result, a significant body of knowledge concerning its physicochemical properties and extensive manufacturing infrastructures already exist[26,28,29] that could be exploited to develop compatible IJP metallization processes.

Electroless (EL) plating provides an attractive alternative to metal nanoparticle sintering for metallization of such thermally sensitive substrates. The EL process involves controlled chemical reduction of metal ions to metal at a surface-immobilized catalyst site, which is carried out at low cost under near ambient, aqueous conditions ideally suited for the manufacturing environment.[30] The deposited EL metal is itself often autocatalytic, permitting continued deposition of metal even after the catalyst site is no longer accessible. Because metal film thickness and continuity can be controlled by varying plating conditions to provide an electrically conductive film, no sintering is necessary. Consequently, given their simplicity and low cost, EL processes are receiving increased attention for IJP patterning of flexible polymer materials.[5,9,11,14−16,31−33]

Recently, we adapted an EL process for IJP-based fabrication of patterned Cu metal films on paper substrates for use as microwave-attenuating materials.[34] In our work, we utilized a commercially available Pd/Sn colloidal catalyst as an ink.

Received: September 26, 2011
Accepted: April 25, 2012
Published: May 7, 2012

Patterns of Pd/Sn ink printed onto paper substrates using a modified inkjet printer were subsequently selectively plated with Cu in a commercial EL Cu plating bath. General properties of the films, including Cu adhesion, feature line edge roughness, and thickness, were determined. Although Cu films exhibiting good pattern fidelity and electrical conductivity were reproducibly obtained, a rather limited range of plating conditions was examined, which precluded a sufficient understanding of the process required for eventual transition to manufacture.

Here we present a more comprehensive study of the influence of 6 plating variables on the deposition of the Cu features according to our process. We utilize a two-level factorial design[35,36] to statistically identify and analyze the effects of each plating variable and its interactions with other plating variables on the measured electrical conductivity of the Cu deposits. A model equation is developed that describes Cu film conductivity as a function of variable levels within the variable ranges investigated and identifies plating conditions for reproducible fabrication of Cu films exhibiting optimal electrical conductivity. The results of our experiments suggest additional process improvements and provide a basis for further development of our metallization process.

EXPERIMENTAL SECTION

A complete description of the experimental procedures and the statistical analysis methods is available in the Supplementary Information. Briefly, line/space patterns having pre-determined fixed dimensions (vide infra, eq 1) were printed on bond or vellum paper (Graytex Papers Inc.) using a Hewlett-Packard Deskjet 9800 Printer in which the cartridge ink had been replaced by Cataposit 44 Pd/Sn colloidal EL catalyst concentrate (Dow Chemical Inc.)[34] After aging for a fixed time under ambient conditions, the Pd/Sn patterned paper was affixed to a custom made sample holder, immersed in a 0.12 M HCl(aq) solution to wet the paper, rinsed in water, and plated in a Fidelity 1025® electroless Cu bath (OMG Fidelity Inc.). The plated sample was rinsed in water, dried at 60°C under ∼1 mm Hg vacuum for 20 min, and stored in a N_2 drybox to inhibit aerial oxidation of the Cu film. The electrical resistance of each Cu line comprising a pattern was measured using an Agilent Model 34401A 6.5 Digit Multimeter operated in the ohmmeter function mode. We varied line dimensions, line spacings, age of the Pd/Sn pattern, type of paper, and EL Cu bath plating time and temperature, with two values selected for each variable, for fabrication of the Cu patterns. Cu plated patterns were fabricated for all possible combinations of these variables, with Cu electrical conductivity, represented as the inverse of the electrical resistance, collectively analyzed as a two-level factorial design using the literature procedure.[35] Variables and variable interactions having a significant effect on conductivity were identified and used to develop and test the model for predicting electrical conductivity.

RESULTS AND DISCUSSION

We performed the work described here with two objectives in mind. First, we wished to determine the effects of various process variables and their interactions on the ability to reproducibly plate Cu patterns having acceptable electrical conductivity for flexible electronics, microwave absorption, and decorative applications using a statistical two-level factorial design method. Second, we sought to use the results obtained to map plating conditions leading to the most economical deposition of such Cu films for transition of our process to a manufacturing environment. On the basis of our previous experience plating paper substrates,[34] we required EL Cu features having an average thickness of at least ∼1.5 micrometers for direct use in such applications. Cu films of this thickness were typically bright red-orange (vellum paper) to darker red-brown (bond paper) in color and exhibited good film homogeneity and acceptable electrical conductivity (i.e., electrical line resistance values of $\leq \sim 0.5\ \Omega\ cm^{-1}$). In addition, such films were sufficiently catalytic for application of Au capping coatings, deposited via EL or galvanic immersion methods,[37,38] that further increase film electrical conductivity, inhibit corrosion, and improve solderability. Our initial goal at this stage of development was the deposition of Cu films having these qualities in times of 20 min or less at lower temperatures (i.e., < 50°C) than those typically used for Cu plating.[39]

Preliminary Experiments. To achieve these objectives, we first performed a series of preliminary experiments to identify appropriate conditions and protocols for carrying out our factorial design work, properly choose variables for study, and determine viable ranges of study for each variable selected. In the course of our initial work, we identified two impediments to successful EL Cu plating of paper substrates. These included inadequate hydration and degraded mechanical stability of the cellulose fiber network comprising the paper substrate during processing, both of which must first be addressed to obtain reproducible EL Cu plating results required for implementation of the factorial design experiments.

Specifically, we find that proper hydration of the cellulose fiber network comprising the paper substrate is a pre-requisite for reproducible EL Cu plating. If a dry sheet of paper bearing a pattern of Pd/Sn colloid ink is immersed in an EL Cu bath, it often plates irregularly and sporadically, if at all. However, if the paper is completely wetted by immersion in water prior to plating, reproducible deposition of EL Cu occurs. The wetting process itself is often non-uniform. Some samples wet completely within a minute or two, as characterized by the near uniform translucence of the well-wetted paper. Other samples are still poorly or only partially wetted even after soaking in water for as long as 30 min. This behavior contrasts with that of dry cellulose microfibrils bearing previously adsorbed Pd/Sn colloid, which directly plate readily and uniformly without pre-wetting.[36,40]

The origin of this phenomenon is uncertain, but restricted surface access in the entangled cellulose fiber mass comprising the paper sheet is certainly expected to influence wetting rates compared to free fibers. It is also known that manufacturers often apply proprietary coatings that can affect wettability during the manufacturing process to improve the properties of paper.[41−43] In addition, lubricants and other materials inadvertently adsorbed during manufacture via processing through automated machinery or handling may also affect wettability, causing it to vary from ream to ream, sheet to sheet, or even among different areas on the same sheet of paper, consistent with our observations.

Regardless of its source, we required a solution to the variable wettability issue to obtain reproducible Cu plating using our process. We observed that the Pd/Sn colloidal ink consistently and completely wetted the dry paper surface without beading or smearing during the printing process. Therefore, we tested the components of the Pd/Sn colloidal dispersion and identified HCl (aq) as an efficient paper wetting agent. Subsequent testing indicated that a 0.12 M HCl (aq) solution completely and consistently wetted our paper samples during a treatment of ∼3 min. After a 2 min rinse in water to remove excess HCl, the wetted paper samples were reproducibly plated in the EL Cu bath.

Decreased mechanical stability of the paper in the EL Cu bath presented an additional problem, especially during plating at higher temperatures. For example, wetted paper samples tended to float to the surface of the Cu bath because of their natural buoyancy, exacerbated by H_2 gas bubble evolution on the paper surface accompanying the Cu deposition. Because Cu plating rates were decreased compared to completely immersed samples, constant manipulations to submerge the samples were necessary. However, these manipulations often led to tearing of the plated sample in or during removal from the Cu bath. Even for paper samples that remained intact, dimensional distortions as large as several millimeters were often observed after plating due to the swelling, stretching, and weakening of the cellulose fiber network of the paper in the Cu bath. These distortions tended to occur primarily, but not exclusively, parallel to the long axis of the paper (i.e., in the direction of the Pd/Sn lines of the block patterns, note Figure 1A and the Supporting Information, Experimental Section), altering the dimensions of the original Pd/Sn line patterns and complicating interpretation of the electrical resistance measurements of the plated Cu lines.

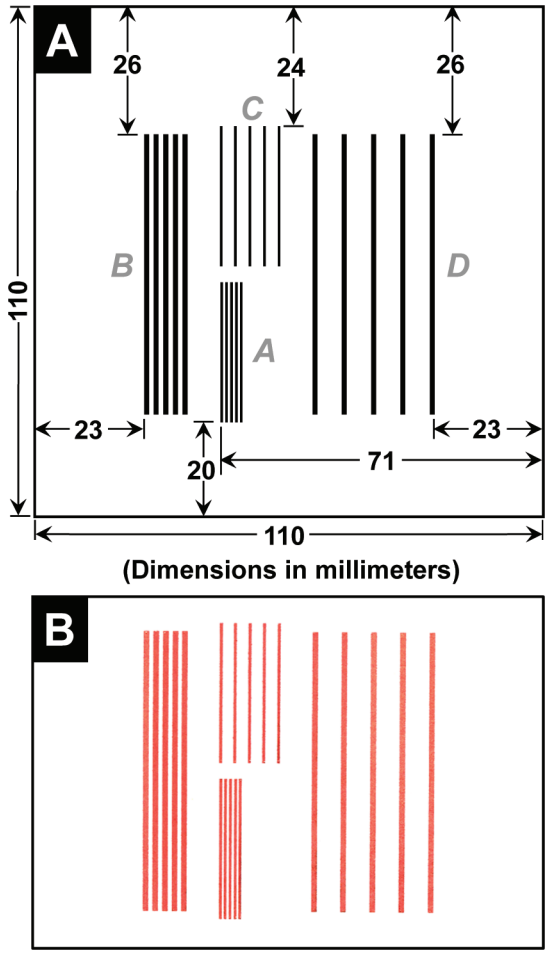

Figure 1. (A) Computer template for the line and space patterns used for the factorial design experiments. (B) Printed colloidal Pd/Sn catalyst pattern after EL Cu plating (conditions: patterned vellum paper aged 21 days and Cu plated 21 min at 42°C).

Therefore, we developed a sample holder to immobilize the paper sheets during processing to minimize handling and control immersion in the Cu bath (see Figure S-1 in the Supporting Information). Paper samples were placed on either side of a PET spacer, then sandwiched between PTFE binder plates that allowed access of the Cu bath to the Pd/Sn patterned paper and clamped together to fix the position of the paper (see the Supporting Information, Experimental Section). Use of this sample holder to treat the paper during the wetting and Cu plating steps eliminated problems associated with incomplete immersion and tearing and greatly minimized, but did not completely eliminate, issues associated with pattern distortions as described later in the text. However, paper samples plated using the sample holder routinely exhibited reproducible and selective Cu deposition, with adherent Cu features (pass Scotch Tape adhesion test) that exhibit invariant electrical resistance values even after flexing the paper, as required for analysis using the factorial design and shown in Figure 1B.

Selection of Variables. Having established an experimental protocol to obtain reproducible EL Cu deposition, we turned our attention to selection of the variables and their ranges for study in the two-level factorial design. On the basis of our experiences, we initially identified nine variables having the potential to affect the Cu plating process and therefore also the electrical resistance of the plated Cu features. These included: (1) fluoboric acid "acceleration" pretreatment of the Pd/Sn patterns prior to EL Cu plating; (2) concentration of the EL Cu bath; (3) surface coverage (i.e., loading) of the Pd/Sn colloidal catalyst on the paper surface; (4) the dimensions (i.e., length and width) of the Pd/Sn catalyst lines on the paper; (5) the spacing of the Pd/Sn catalyst lines on the paper; (6) the type of paper plated; (7) the age of the Pd/Sn catalyst lines; (8) plating time in the EL Cu bath, and; (9) the temperature of the EL Cu bath.

Among these factors, three were quickly eliminated from further consideration because they were found to induce irreproducible Cu deposition during preliminary experiments. For example, the colloidal Pd/Sn electroless catalyst used here comprises a Pd(0) rich core surrounded by a β-stannic shell containing both Sn(II) and Sn(IV) species.[30] The shell functions to maintain the Pd(0) core in the catalytic zerovalent state and provides adhesion of the colloid to the surface to be plated. However, it also limits access of the EL bath to the catalytic Pd(0) core, inhibiting the EL metal deposition rate. Access to the Pd(0) core can be improved by partial dissolution of the β-stannic shell via treatment with fluoboric acid in a process known as "acceleration", which promotes increased EL plating rates. Acceleration must be carefully controlled to prevent dissolution of that portion of the β-stannic shell anchoring the catalyst to the substrate because dislodged Pd/Sn colloids can redeposit elsewhere on the substrate, leading to nonselective Cu deposition. In addition, dislodged Pd/Sn colloids can also function as catalyst seeds in the EL Cu solution, promoting undesirable autocatalytic decomposition of the EL Cu bath leading to bulk precipitation of Cu metal from the bath.

In fact, our preliminary attempts to enhance EL Cu plating rates on our paper substrates using such acceleration pretreatments routinely produced Cu plated samples exhibiting evidence of non-selective Cu deposition. Noticeable line broadening during Cu plating of the Pd/Sn patterns was often observed, together with a pale red patina on the non-plated portions of the paper (e.g., note Figure S-2 in the Supporting Information). Careful examination of the patina indicated the presence of fine Cu microparticles embedded in

Table 1. Two-Level Factorial Design Results Summary

row[a]	L^b	S^c	P^d	A^e	T^f	H^g	$1/R$ $(\Omega^{-1})^h$	effect E $(\Omega^{-1})^i$	ID[j]	S^k
1	−1	−1	−1	−1	−1	−1	0.402576	0.679872	average[l]	
2	+1	−1	−1	−1	−1	−1	0.456204	0.051247	L	
3	−1	+1	−1	−1	−1	−1	0.410509	0.000141	S	
4	+1	+1	−1	−1	−1	−1	0.419111	−0.01888	LS	
5	−1	−1	+1	−1	−1	−1	0.093041	−0.27816	P	yes
6	+1	−1	+1	−1	−1	−1	0.043011	−0.0708	LP	yes
7	−1	+1	+1	−1	−1	−1	0.259605	0.167344	SP	yes
8	+1	+1	+1	−1	−1	−1	0.216263	−0.02565	LSP	
9	−1	−1	−1	+1	−1	−1	0.572082	0.031733	A	
10	+1	−1	−1	+1	−1	−1	0.718391	0.01318	LA	
11	−1	+1	−1	+1	−1	−1	0.445633	0.018332	SA	
12	+1	+1	−1	+1	−1	−1	0.501002	−0.00721	LSA	
13	−1	−1	+1	+1	−1	−1	0.000099	−0.09034	PA	yes
14	+1	−1	+1	+1	−1	−1	0.162920	0.015844	LPA	
15	−1	+1	+1	+1	−1	−1	0.199840	0.004914	SPA	
16	+1	+1	+1	+1	−1	−1	0.097867	−0.00516	LSPA	
17	−1	−1	−1	−1	+1	−1	0.801282	0.492354	T	yes
18	+1	−1	−1	−1	+1	−1	0.829187	−0.05366	LT	
19	−1	+1	−1	−1	+1	−1	0.691563	0.010241	ST	
20	+1	+1	−1	−1	+1	−1	0.556174	0.021287	LST	
21	−1	−1	+1	−1	+1	−1	0.484027	−0.04034	PT	
22	+1	−1	+1	−1	+1	−1	0.431779	0.047694	LPT	
23	−1	+1	+1	−1	+1	−1	0.640205	0.001687	SPT	
24	+1	+1	+1	−1	+1	−1	0.574713	−0.0023	LSPT	
25	−1	−1	−1	+1	+1	−1	1.020408	−0.00422	AT	
26	+1	−1	−1	+1	+1	−1	0.976563	−0.03489	LAT	
27	−1	+1	−1	+1	+1	−1	0.992063	0.015629	SAT	
28	+1	+1	−1	+1	+1	−1	0.978474	−0.00291	LSAT	
29	−1	−1	+1	+1	+1	−1	0.348918	−0.01541	PAT	
30	+1	−1	+1	+1	+1	−1	0.335121	0.029767	LPAT	
31	−1	+1	+1	+1	+1	−1	0.604595	0.000805	SPAT	
32	+1	+1	+1	+1	+1	−1	0.551268	0.01097	LSPAT	
33	−1	−1	−1	−1	−1	+1	0.576037	0.371339	H	yes
34	+1	−1	−1	−1	−1	+1	0.902527	0.058647	LH	yes
35	−1	+1	−1	−1	−1	+1	0.276702	−0.02881	SH	
36	+1	+1	−1	−1	−1	+1	0.533618	0.01736	LSH	
37	−1	−1	+1	−1	−1	+1	0.431406	0.079837	PH	yes
38	+1	−1	+1	−1	−1	+1	0.472144	−0.05103	LPH	
39	−1	+1	+1	−1	−1	+1	0.648508	0.040619	SPH	
40	+1	+1	+1	−1	−1	+1	0.510204	−0.02303	LSPH	
41	−1	−1	−1	+1	−1	+1	0.530786	−0.04302	AH	
42	+1	−1	−1	+1	−1	+1	0.965251	−0.01147	LAH	
43	−1	+1	−1	+1	−1	+1	0.312891	0.017757	SAH	
44	+1	+1	−1	+1	−1	+1	0.818331	0.002176	LSAH	
45	−1	−1	+1	+1	−1	+1	0.323625	0.039661	PAH	
46	+1	−1	+1	+1	−1	+1	0.369822	0.014886	LPAH	
47	−1	+1	+1	+1	−1	+1	0.616523	0.009541	SPAH	
48	+1	+1	+1	+1	−1	+1	0.591716	0.022677	LSPAH	
49	−1	−1	−1	−1	+1	+1	1.381215	0.128718	TH	yes
50	+1	−1	−1	−1	+1	+1	1.436782	−0.01734	LTH	
51	−1	+1	−1	−1	+1	+1	1.02459	−0.00603	STH	
52	+1	+1	−1	−1	+1	+1	1.428571	0.008271	LSTH	
53	−1	−1	+1	−1	+1	+1	1.01626	−0.03896	PTH	
54	+1	−1	+1	−1	+1	+1	1.012146	0.030413	LPTH	
55	−1	+1	+1	−1	+1	+1	1.182033	−0.0191	SPTH	
56	+1	+1	+1	−1	+1	+1	1.106195	−0.01495	LSPTH	
57	−1	−1	−1	+1	+1	+1	1.474926	−0.02928	ATH	
58	+1	−1	−1	+1	+1	+1	1.396648	−0.02283	LATH	
59	−1	+1	−1	+1	+1	+1	1.213592	−0.04992	SATH	
60	+1	+1	−1	+1	+1	+1	1.162791	−0.0332	LSATH	
61	−1	−1	+1	+1	+1	+1	0.859107	0.027101	PATH	

dx.doi.org/10.1021/am3006934 | ACS Appl. Mater. Interfaces 2012, 4, 2358−2368

Table 1. continued

row[a]	L^b	S^c	P^d	A^e	T^f	H^g	$1/R$ $(\Omega^{-1})^h$	effect E $(\Omega^{-1})^i$	ID[j]	S^k
62	+1	−1	+1	+1	+1	+1	0.929368	0.030655	LPATH	
63	−1	+1	+1	+1	+1	+1	1.101322	0.019126	SPATH	
64	+1	+1	+1	+1	+1	+1	1.091703	0.010611	LSPATH	

[a]Experiment number. [b]Coded length/width (L/W) ratio of Cu line in each pattern block. $L = -1 \equiv L/W = 95$ mm/0.48 mm and $L = +1 \equiv L/W =$ 190 mm/0.98 mm. [c]Coded spacing of Cu lines in each pattern block. $S = -1 \equiv$ spacing equal to linewidth, W, and $S = +1 \equiv$ spacing equal to five times linewidth, 5 W. [d]Coded designation of paper type. $P = -1 \equiv$ vellum paper and $\boldsymbol{P} = +1 \equiv$ bond paper. [e]Coded designation for age of the printed Pd/Sn colloidal catalyst patterns prior to EL Cu plating. $A = -1 \equiv 7$ days old and $\boldsymbol{A} = +1 \equiv 21$ days old. Pd/Sn catalyst patterned papers were aged on an office desk in the air under fluorescent lighting until needed for experiments. [f]Coded designations for EL Cu plating times. $T = -1 \equiv 14$ min and $T = +1 \equiv 21$ min. [g]Coded designation for the temperature of the EL Cu bath during plating. $H = -1 \equiv 34$°C and $H = +1 \equiv 42$°C. [h]Reciprocal resistance value (Ω^{-1}) calculated as the inverse of the average resistance, R (Ω), determined from the individual resistance values measured for the 5 Cu lines comprising a given block in the pattern shown in Figure 1 and designated by the levels of the L and S coded variables in this table. Consult the Supporting Information, Table S-1, for individual measured resistance values and the average R value used in each calculation. [i]Effect (Ω^{-1}) due to the variable or combination of variables indicated in column 8 of this table as calculated from the ($1/R$) values of column 9 using Yates' Algorithm in the Supporting Information, Table S-2. [j]Identification of the variable or combination of variables responsible for the effect resulting from the experiment indicated by the variable levels in the table row. The variable or combination of variables is represented by the +1 entries in the table row. [k]Significance: Identification of the effects from column 10 having a real effect on the electrical conductivity of the Cu films as described in the text. "Yes" ≡ variable or combination of variables from column 8 significantly influences Cu film conductivity. Effects from all other variables or combinations of variables reflect random error. [l]Grand average ($1/R$) response of the system within the ranges of all variables examined.

the paper, consistent with diffusion and re-deposition of Pd/Sn colloid dislodged from the catalyst patterns. This problem was exacerbated as plating times and temperatures were increased. It was also occasionally accompanied by sudden bulk Cu deposition onto the sample due to rapid autocatalytic decomposition of the Cu bath. Therefore, given the process irreproducibility associated with these plating non-selectivity and Cu bath stability issues, we abandoned acceleration pretreatment as a variable for consideration in the factorial design.

Increases in the concentration of the EL Cu bath were also expected to increase Cu plating rates. Therefore, we prepared and tested EL Cu baths having component concentrations up to twice those recommended by the manufacturer. However, once again irreproducible Cu plating results were observed. Although Cu plating rates were enhanced, as expected, plating non-selectivity and EL Cu bath stability issues similar to those noted with the use of the accelerator pretreatments were observed. Consequently, we elected to use a Cu bath prepared according to the manufacturer's instructions for all experiments and forgo further consideration of the concentration of the EL Cu bath as a variable in the factorial design.

Cu bath instability and autocatalytic decomposition issues were also noted during attempts to enhance Cu plating rates by increasing the Pd/Sn catalyst loading on the paper. For example, we successfully increased Pd/Sn surface loading by overwriting existing Pd/Sn catalyst lines on paper samples using the printer. No line registration issues were observed for features having the dimensions considered here (note Figure 1A)[34] and deposition of the additional Pd/Sn catalyst was evidenced by darkening of the brown line color. However, during subsequent Cu plating autocatalytic decomposition of the Cu bath was observed, consistent with release of Pd/Sn colloid seeds from the paper into the bath solution. This behavior suggested that Pd/Sn surface coverage was essentially complete during the first printing cycle and that Pd/Sn colloids deposited during the second print cycle were weakly adsorbed to the underlying Pd/Sn colloids, rather than the cellulose fibers of the paper. Therefore, we did not consider Pd/Sn loadings as a viable factor for further investigation in the factorial design.

Among the other variables considered, no selectivity or bath stability issues were noted and reproducible Cu deposition was maintained. Therefore, we selected the remaining six variables for investigation using the factorial design. In particular, we chose the length/width ratio (L/W) defining each printed Pd/Sn catalyst line and the line spacing, hereafter designated by L and S, respectively, as variables to assess the effect of feature geometry, if any, in our Cu plating process. Specifically, four blocks of Pd/Sn lines, each containing five lines of equal length and width with fixed line spacing, were printed as described in detail in the Supporting Information Experimental Section and shown in Figure 1A. In terms of designations appropriate for the factorial analysis, a line coded $L = -1$ had an L/W ratio of 30.5 mm/0.48 mm, while one coded $L = +1$ had an L/W ratio = 61.0 mm/0.96 mm. Line spacing coded $S = -1$ corresponded to spacing equal to the linewidth, (i.e., $W = 0.48$ mm or 0.96 mm), whereas $S = +1$ indicated spacing equivalent to five times the linewidth (i.e., $5W = 2.40$ mm or 4.80 mm). Therefore, the four blocks described each of the four possible combinations of coded (L, S) values, i.e., Block A = (−1, −1), Block B (+1, −1), Block C (−1, +1), and Block D (+1, +1).

Our choices of line dimensions, L, are dictated by eq 1, which describes the electrical resistance expected for a Cu metal line of resistivity, ρ ($= 1.68 \times 10^{-8}$ Ω m),[44] having a rectangular cross section with length, L, width, W, and thickness, h.

$$R = \rho L/(Wh) \quad (1)$$

Because both the length (L) and width (W) of the longer lines (i.e., coded $\boldsymbol{L} = +1$) in Figure 1A are *each* exactly twice those of the shorter lines (i.e., coded $L = -1$), eq 1 indicates that identical Cu thicknesses and measured resistance values are ideally expected for all lines in the absence of any real effects during Cu plating due to the variables studied (vide infra, Table 1). However, changes in Cu plating rates as the levels of any significant experimental variables are changed will lead to different line thicknesses, and therefore also different measured electrical resistances. Therefore, our selection provides a baseline against which changes in electrical resistance associated with the influence of the variables studied, as determined from the analysis of the factorial design, can be gauged.

The type of paper used, P, is one such variable expected to influence the Cu plating process. For example, factors such as

paper roughness and porosity are expected to affect not only the amount (*i.e.*, surface coverage) of the Pd/Sn catalyst bound, but also its accessibility to the EL Cu solution during plating. Because plating initiates and proceeds in an isotropic fashion from each Pd/Sn site,[30] any differences in Pd/Sn seed surface coverage or solution accessibility must ultimately influence the quantity of Cu deposited and its electrical resistance. Therefore, we have chosen both vellum paper and bond paper, arbitrarily coded $P = -1$ and $P = +1$ in the factorial design, respectively, for study in our experiments. The more tightly cross-linked cellulose fiber network in the vellum paper provides a smoother and less porous surface compared to the bond paper.

The age of the Pd/Sn catalyst lines printed on the paper, ***A***, is yet another variable potentially affecting the Cu deposition process. The Pd/Sn colloid initially deposited onto the paper during the pattern printing process slowly oxidizes in the air with increased time. Although oxidation of Sn(II) to Sn(IV) and Pd(0) to Pd(II) both occur, Pd(II) is rapidly re-reduced to Pd(0) by any Sn(II) present until Sn(II) levels are depleted. Thereafter, irreversible oxidation of Pd(0) to Pd(II) can occur.[30] Consequently, an induction period during which Pd(II) is first reduced back to catalytically active Pd(0) is observed prior to initiation of Cu plating. During this reduction, a portion of the nascent Pd(0) atoms produced diffuse from the colloid adsorption site[45,46] and may be re-adsorbed onto the nearby surface, where they can promote EL Cu deposition.

The delay in initiation of Cu plating and the re-adsorption of released Pd(0) can each influence the morphology of the deposited Cu. Therefore, in order to develop a reliable process providing the most uniform Cu features, Cu plating should be done immediately after printing the Pd/Sn catalyst patterns or at a time after colloid oxidation to Pd(II) is essentially complete. Because plating of freshly printed Pd/Sn catalyst patterns may not always be possible or convenient, we have selected Pd/Sn catalyst line aging times of 7 days (i.e., $A = -1$) and 21 days (i.e., $A = +1$) for investigation. These selections provide an opportunity to determine whether oxidation of the Pd/Sn colloid adsorbed to the paper is sufficiently complete to ensure that catalyst line age does not influence the amount of Cu deposited.[30]

Plating time, *T*, and plating temperature, *H*, have long been known to affect the quantity and quality of EL Cu deposits[39] and are natural selections as variables for study in our system. The amount of Cu plated generally increases with both plating time and temperature, though plating selectivity and bath stability issues can become important considerations as well. Our choices for these variables reflect the limitations of the Fidelity 1025® EL Cu bath and our objective of plating Cu features exhibiting acceptable electrical resistances in times of ~20 min or less at a temperature <50°C (vide supra). Although the Fidelity 1025® EL Cu bath efficiently deposits Cu at temperatures near or slightly above room temperature, autocatalytic decomposition of the bath usually occurs at temperatures > ~45°C during plating of our samples. In contrast, successful deposition of Cu films occurs on our Pd/Sn patterned substrates at room temperature, though plating times in excess of 30 min are required to obtain features having acceptable electrical resistance. Therefore, in order to span a reasonable temperature range for study we assign the $H = -1$ and $H = +1$ levels in the factorial design to EL Cu baths operated at 34 and 42°C, respectively. Plating times of 14 min and 21 min are assigned for the $T = -1$ and $T = +1$ levels, respectively, consistent with our objective of limiting plating time to ~20 min or less.

Factorial Analysis Results. Table 1 summarizes the results of the experiments associated with the factorial design analysis. Columns 2-7 summarize the levels of each of the *L*, *S*, *P*, *A*, *T*, and *H* variables corresponding to the experiments described by each row from column 1. Note that every set of 4 consecutive rows in Table 1 corresponds to results obtained from a single piece of block patterned paper per our definition of the *L* and *S* variables in Figure 1. Entries in column 8 are $(1/R)$ values, calculated as the inverse of the average resistance of the 5 Cu lines comprising each pattern block in Figure 1 (note Table S-1 in the Supporting Information for electrical resistance data), which provide a convenient approximation of Cu film conductivity sufficient for our purposes. The use of the $(1/R)$, rather than the average *R* values, obviates data distortions resulting from previously described[34] critical phase behavior (i.e., limited or partial Cu particle connectivity resulting in high line resistance) for these systems, which is also observed in certain experiments here (note Table S-1 in the Supporting Information). In addition, the $(1/R)$ values provide a convenient means to map and identify optimal plating conditions in terms of large $(1/R)$ values associated with plating conditions leading to fabrication of highly conductive Cu lines, as described in the next section.

Column 9 summarizes the effects from each experiment, calculated via Yates' Algorithm analysis of the $(1/R)$ as described in Table S-2 in the Supporting Information. The variable or combination of variables associated with each effect is listed in column 10 and those having significant (i.e., real) effects on the $(1/R)$ are shown in column 11. Factors deemed significant in column 11 are identified from the normal probability plot shown in Figure 2, in which effects are plotted in order from smallest to largest against their probability of occurring randomly (see Table S-3 in the Supporting Information). The effects due to random error constitute a

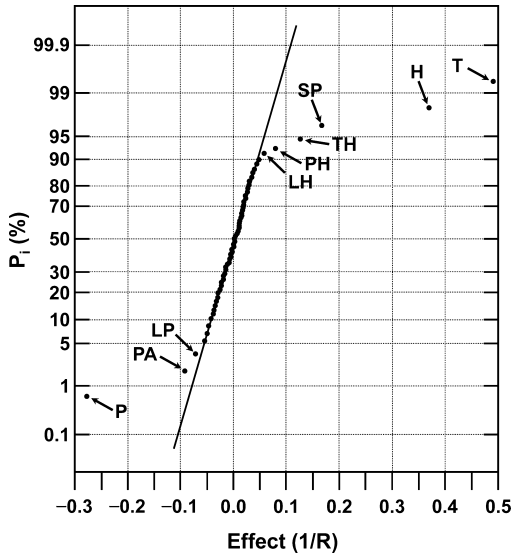

Figure 2. Normal probability plot of effects. Significant effects are indicated by points deviating from the straight line defined by effects attributed to random error. The data were taken from Table S-3 in the Supporting Information. Variable(s) associated with each significant effect are identified by one or more letters according to the nomenclature of Table 1.

dx.doi.org/10.1021/am3006934 | ACS Appl. Mater. Interfaces 2012, 4, 2358−2368

straight line characteristic of a normal error distribution, whereas factors significantly influencing the $(1/R)$ deviate from that line.[35]

Significant effects and variables, together with the grand average response (i.e., 0.679872) in Table 1, describe a model shown in eq 2 for the estimation of the $(1/R)$ within the coded −1 to +1 ranges of the six variables examined here.

$$(1/R)_{est} = 0.679872 + 0.5(0.492354T + 0.371339H + 0.167344SP + 0.128718TH + 0.079837PH + 0.058647LH - 0.27816P - 0.09034PA - 0.0708LP) \quad (2)$$

The estimated $(1/R)$ values, i.e., $(1/R)_{est}$, are calculated according to eq 2 as deviations from the grand average weighted by the product of the sign and magnitude of each significant effect and the coded values of each of its corresponding factors. Equation 2 can be used to calculate the $(1/R)_{est}$ values for each of the experimental conditions in Table 1, as summarized in Table S-4 in the Supporting Information. A residual, $\Delta(1/R)$, which provides a measure of the ability of the model to accurately predict the $(1/R)$, is calculated from the corresponding observed $(1/R)$, i.e., $(1/R)_{obs}$, and $(1/R)_{est}$ values according to eq 3.

$$\Delta(1/R) = (1/R)_{est} - (1/R)_{obs} \quad (3)$$

A normal probability plot of the $\Delta(1/R)$, in which the residuals are plotted in order from smallest to largest against their probability of occurring (see Table S-5 in the Supporting Information), is shown in Figure 3A. The plot yields a straight line approximately symmetric about $\Delta(1/R) = 0$, indicating that eq 2 provides a reasonable model for estimation of the $(1/R)$ values within the ranges of the variables investigated here.

Further examination of the results shown in Table 1 and Figure 2 reveals a number of important points concerning our system. For example, among the six variables studied the plating time, *T*, Cu bath temperature, *H*, and type of paper, *P*, together clearly exert the largest effect on the electrical conductivity of the Cu features, as measured by the $(1/R)$. It is not surprising that positive effects on the $(1/R)$ are associated with the *T* and *H* variables, as increases in either factor enhance both the plating rate and the amount of Cu deposited. Their effects are not independent, however, but are reinforced by the modest positive synergistic interaction represented by the *TH* interaction term.

Similarly, there is a substantial negative influence on the $(1/R)$ due to the type of paper used, *P*, with the rougher more porous bond paper generally yielding smaller $(1/R)$ than vellum paper under otherwise identical plating conditions. Such behavior is consistent with expectations of lower Pd/Sn catalyst loading levels on the more loosely packed cellulose network of the bond paper, resulting in increased times compared to vellum paper to establish the Cu particle connectivity required to form the thick Cu films exhibiting good electrical conductivity.[34] This result clearly indicates that characteristics of the paper play an important role in determining the quality of the plated Cu features and must be considered during the design phase for a given application.

We also note that the $(1/R)$ are not directly influenced by the age of the Pd/Sn catalyst lines (i.e., *A*) or the nature of the printed features (i.e., *L* and *S*) over the ranges studied for these variables, though lesser influences due to the *PA* interaction and

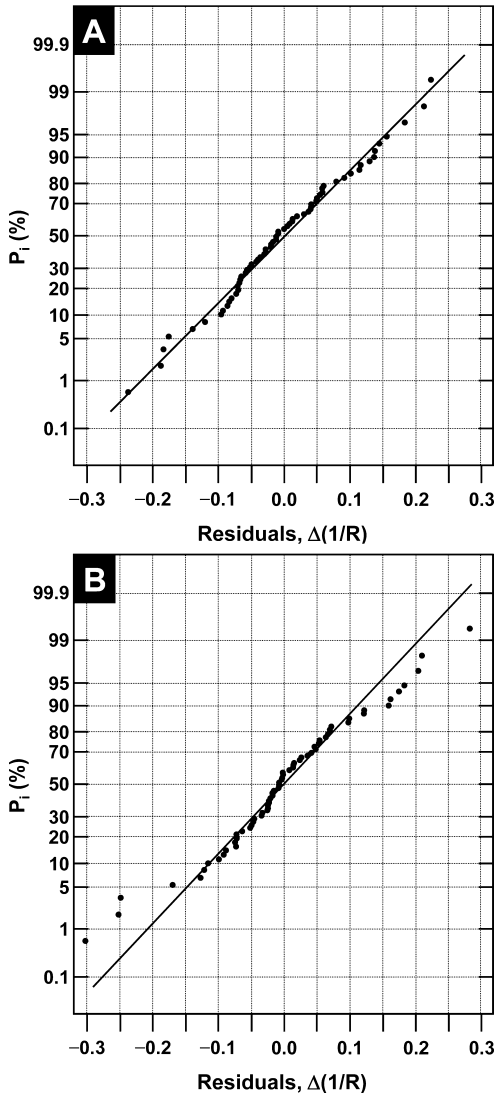

Figure 3. Residuals probability plots. (A) $\Delta(1/R)$ calculated from the model of eq 2. (B) $\Delta(1/R)$ plotted with omission of *LH* and *LP* terms in eq 2. See Tables S-5 and S-7 in the Supporting Information for data.

LP, *LH*, and *SP* interactions, respectively, do occur. These results are in agreement with known behavior of the Pd/Sn catalyst[30] and our expectations based on our choices of limits for these variables. For example, we note from our experience that aerial oxidation of Pd/Sn to Pd(II) and Sn(IV) is typically complete within a few days. Therefore, little difference between Pd/Sn patterned paper samples aged 7 days and 21 days prior to plating is expected, consistent with the observed lack of an effect due to *A* on the $(1/R)$. Similarly, our choice of feature line dimensions is dictated by eq 1, with the goal of providing Cu features ideally exhibiting identical electrical conductivities (vide supra). In addition, although plating dependencies on feature spacing can occur for sub-micrometer features, where diffusion effects and anomalies become important,[47−52] such effects are typically not observed for the macroscopic features and line spacings selected for study here. Therefore we expect the $(1/R)$ to be independent of both *L* and *S*, as confirmed by our analysis and model.

Although Cu conductivity is determined primarily by the major effects associated with the *T*, *H*, and *P* variables in eq 2, contributions from the various two factor interactions also

occur. For example, Figure 3B illustrates a normal probability plot of the residuals obtained when the positive *LH* and negative *LP* interaction terms are omitted from eq 2 (see Tables S-6 and S-7 in the Supporting Information). These terms are associated with the smallest interaction effects. However, their omission substantially degrades the quality of the residuals plot in Figure 3B. Linearity is noticeably compromised, especially at the extrema, and slight asymmetry about the $\Delta(1/R) = 0$ point is noted, consistent with a model that inadequately describes the system.

Finally, it is interesting to note that, with the exception of the *TH* and *LH* interactions, the remaining interactions are all associated with the *P* term. This behavior suggests that small distortions of the cellulose networks of the papers may persist during the plating process, despite our use of the sample holder. This argument is supported by careful examination of the Cu lines after completion of the plating process. For example, in some cases measurements of Cu line lengths exceed those of the printed Pd/Sn catalyst by as much as ~0.6 mm, especially for samples plated at the higher temperature and longer times. In addition, distortions in the form of slight Cu line curvature are also occasionally observed. While our results are insufficient to definitively assign physicochemical interpretations for these interaction terms, it is clear that further processing improvements related to sample manipulation during the plating process will be required, especially for applications requiring smaller Cu feature sizes than those tested here.

Mapping. Although the model of eq 2 provides a quantitative description of our system, geometric representations often provide a more convenient means to visualize the major response trends.[35] Figure 4 provides one such

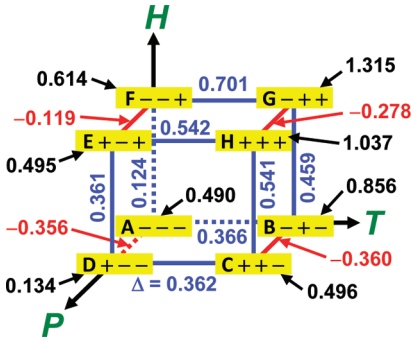

Figure 4. Average $1/R$ response map. Geometric representation of the average influence of the *P*, *T*, and *H* variables on the $(1/R)$ in Ω^{-1} as described in the text.

representation in terms of the average variations expected in the $(1/R)$ with the *P*, *T*, and *H* parameters. In this case, the *P*, *T*, and *H* variables form a set of mutually orthogonal axes defining a cube. The vertices of the cube are identified by a capital letter and a sequence of three consecutive "+" and/or "−" symbols representing the levels of the *P*, *T*, and *H* variables, respectively. For example, the A(− − −) and E(+ − +) vertices represent conditions where $P = T = H = -1$ and $P = H = +1$ with $T = -1$, respectively. Values in black text at each vertex represent the average (1/R) associated with the specific *P*, *T*, *H* levels at that vertex, with the average calculated over all ±1 levels of the *L*, *S*, and *A* variables in Table 1. For example, the $(1/R) = 0.490\ \Omega^{-1}$ at vertex A is calculated as the average of all $(1/R)_{obs}$ in Table 1 for which $P = T = H = -1$ (i.e., $(1/R)_{obs}$ from rows 1−4 and 9−12, inclusive). Similarly, the (1/R) = $0.495\ \Omega^{-1}$ value at vertex E is the average of all the $(1/R)_{obs}$ for which $P = H = +1$ with $T = -1$ (i.e., $(1/R)_{obs}$ from rows 37-40 and 45-48, inclusive). Differences between adjacent vertices correspond to changes in $(1/R)$ occurring as the variable associated with the axis is changed from its −1 to +1 value. These changes are shown as numerical "Δ-values" along the edges of the cube, with blue and red values and cube edges corresponding to increases and decreases, respectively, in the average $(1/R)$. For example, edge EH represents an average increase in $(1/R)$ of $0.542\ \Omega^{-1}$ as *T* is changed from its −1 to +1 level at fixed $P = H = +1$, whereas edge AD indicates an average decrease in $(1/R)$ (i.e., $-0.356\ \Omega^{-1}$) as *P* is changed from its −1 to +1 level at fixed $T = H = -1$.

Note that averaging in this manner is necessary to summarize the complex form of eq 2 in terms of a single simple geometric 3D representation in Figure 4. However, the simplification inherent in the averaging process leads to loss of detailed information associated with the various significant (though smaller) interaction terms in eq 2 containing the *L*, *S*, and *A* factors. Nevertheless, the geometric representation does provide a useful overview that captures the behavior of the main effects in our system, consistent with the dominance of the *P*, *T*, and *H* terms in controlling the Cu feature plating and conductivity. For example, cube face ABGF in Figure 4 summarizes the behavior of the vellum paper (i.e., $P = -1$) as *T* and/or *H* are changed. Large values for the average (1/R) are noted at each vertex, together with positive Δ-values, consistent with strong contributions due to both the *T* and *H* variables and the *TH* interaction, as expected from the model of eq 2. Similar behavior is noted for cube face DCHE, which summarizes the influences of *T* and/or *H* on the bond paper (i.e., $P = +1$). In this case, the average $(1/R)$ value at each vertex is less than the value at the corresponding vertex representing the vellum paper (cf., D vs. A, C vs. B, H vs. G, and E vs. F). As a result, Δ-values for each of the AD, BC, GH, and FE edges representing the $P = -1$ to +1 transitions at the various combinations of *T* and *H* levels are negative, which illustrates the large negative *P* effect in our system.

Examination of the trends represented in Figure 4 clearly indicates that use of vellum paper provides an advantage over bond paper for the fabrication of high quality Cu patterns. The most conductive Cu patterns are expected for vellum by plating for the longer time in the higher temperature Cu bath (i.e., vertex G; $(1/R) = 1.315\ \Omega^{-1}$), consistent with the dominant positive effects associated with the *T* and *H* variables. Cu patterns having appreciable conductivity are also expected for samples plated at the longer time in the lower temperature Cu bath (i.e., vertex B; $(1/R) = 0.856\ \Omega^{-1}$). In contrast, the most conductive Cu patterns on bond paper require use of the higher temperature Cu bath and longer plating time (i.e., vertex H; $(1/R) = 1.037\ \Omega^{-1}$); use of either the shorter plating time (i.e., vertex E; $(1/R) = 0.495\ \Omega^{-1}$) or the lower temperature bath (i.e., vertex C; $(1/R) = 0.496\ \Omega^{-1}$) drastically reduce the $(1/R)$.

Despite these restrictions, however, quality Cu features can be fabricated on the bond paper. For example, Figure 5 shows an array of Cu split-ring resonators useful for microwave attenuation applications prepared by plating printed Pd/Sn patterns aged ~2 years on bond paper for 19 min in a 38°C Cu bath. These conditions are near those defined by vertex H in Figure 4, yet satisfy our stated goal of plating samples in <20 min. Although these features are circular, rather than linear, their widths and spacing are comparable to the ranges defined here by our line structures. Careful examination of Figure 5

dx.doi.org/10.1021/am3006934 | ACS Appl. Mater. Interfaces 2012, 4, 2358−2368

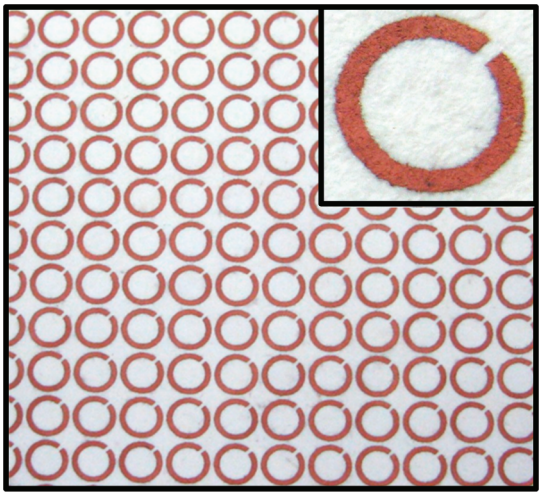

Figure 5. Cu plated split-ring resonators. Arrays of EL Cu resonator structures on bond paper prepared as described in the text. The Pd/Sn patterns on the paper were aged ~2 years prior to Cu plating. The outside diameter of each resonator is ~4.5 mm (14 points) with a Cu linewidth of ~0.48 mm (1.5 points) and a gap of ~0.32 mm (1 point). Electrical resistance measurements of ≤1 Ω are measured for each resonator from the edges of its gap. Insert: Close-up view of an individual Cu resonator.

indicates that Cu plating occurs selectively at the Pd/Sn patterned sites. Plating readily occurs despite the ~2 year age of the Pd/Sn patterns, attesting to their stability during extended storage under ambient conditions and providing a lower estimate for their shelf life. Although some variation in Cu linewidth consistent with the roughness of the paper surface is noted (Figure 5, inset), plating is otherwise uniform and reproducible across the entire array of features. The plating uniformity is reflected in the electrical resistance of the Cu features, with measurements from 15 randomly chosen resonators yielding an average resistance of 0.92 Ω, a standard deviation of 0.04 Ω, and a range of 0.86−1.00 Ω. These values are in good agreement with our targeted resistance of ≤1 Ω for resonators of this size for effective microwave attenuation.[34] This behavior confirms that such structures can be readily fabricated using the design guidelines of Figure 4 and our model in eq 2 under process conditions (i.e., < 20 min plating time at temperatures <50°C) amenable to efficient manufacture.

CONCLUDING REMARKS

In conclusion, we have described a method for selective electroless deposition of metals such as Cu onto paper inkjet patterned with a colloidal Pd/Sn electroless catalyst. Good quality Cu films exhibiting low electrical resistance are reproducibly and uniformly deposited onto Pd/Sn patterns as old as ~2 years using the method. A statistical analysis of Cu patterns prepared according to our method using a two-level factorial design indicates that the electrical conductivity of the films is governed predominantly by the plating time (T), plating temperature (H), and type of paper (P) used. We observe no direct dependence of the conductivity on the feature dimensions (i.e., line dimensions (L) and spacing (S)) or age of the Pd/Sn patterns (A) for the ranges of the variables studied, although various two-factor interactions containing these terms are present and do influence the measured conductivity to a lesser degree. Conductivity of the plated Cu features is enhanced as either or both T or/and H are increased, as expected, but decreases with an increase in P, corresponding to use of paper having increased roughness and porosity. A model derived from the factorial analysis provides a means to predict and optimize Cu film conductivity within the ranges of the variables studied and identifies areas for further process improvement.

With regard to the latter point, further improvements of our process will be dictated by successfully addressing two key issues identified from our model and experiments. First, although our use of a sample holder minimizes tearing and distortions of the paper substrate during processing, it does not completely eliminate these problems. Some swelling of the paper sheets during plating still occurs, which is observed as slight distortions of our Cu patterns. Pattern distortion, together with paper morphology and technological limitations of the inkjet printer, ultimately determines the resolution of the Cu features[34] that can be fabricated. While printer technology improvements are beyond the scope of our work, smoother papers exhibiting well controlled porosities are becoming available through the use of papers prepared from nanocellulose fibers.[43,53−56] Minimization of pattern distortions will require investigation of chemical cross-linking[41,57−63] approaches to strengthen the cellulose fiber network of the paper or use of polymer reinforced paper composites[64−66] as substrates. Preliminary experiments with polymer reinforced papers (*e.g.*, "Ruff-N-Tuff" ™ Tear Resistant Paper, Graytex Papers Inc.) in our laboratory indicate that pattern distortion is indeed inhibited compared to conventional paper, confirming the viability of this approach.

The second issue concerns the stability of the bound Pd/Sn catalyst during sample processing and plating. Although the Cu films prepared here are well-adhered due to their comingling with the cellulose fibers of the paper,[34] the colloidal Pd/Sn catalyst particles are more weakly bound.[30] Therefore, sufficient desorption of Pd/Sn colloid from the paper during plating can overwhelm the ability of bath inhibitors to neutralize their catalytic activity, eventually seeding Cu microparticle formation in the Cu bath. As shown in Figure S-2 in the Supporting Information, the presence of unbound Pd/Sn colloids and Cu microparticles in the Cu bath promotes (1) non-selective Cu deposition when the Cu microparticles are subsequently randomly adsorbed onto the paper and (2) autocatalytic decomposition of the EL Cu bath. Such effects are clearly counterproductive, leading to decreased process efficiency and increased costs.

We have previously demonstrated that Sn-free Pd colloids[45,46,67] can be strongly adhered to surfaces bearing amine-based ligands via covalent bond formation. Various alkylamines (e.g., ethylenediamine[68,69] or benzylamine[70−72]) and heteroaromatic amines (e.g., pyridine[73−76]) strongly bind Pd(II) colloids and sufficiently stabilize their catalytic Pd(0) state[30,71] for efficient catalysis of the EL metal deposition process. The use of cellulose paper materials bearing grafted amine functional groups[41,77] or amine polymer-cellulose composites[55,64,66] as substrates, in combination with Sn-free Pd species,[16,45,46,67,71,78−82] is expected to further reduce the deleterious effects associated with Pd loss from the surface during plating and eliminate the need for the environmentally unfriendly adhesive Sn component of the Pd/Sn colloid.[30] We are currently working to apply such chemistries to our paper substrates, understand the factors that determine metal quality and feature resolution on the modified substrates, and extend

our process to encompass related direct-write EL plating techniques not requiring Pd catalysts.[14,83−85]

■ ASSOCIATED CONTENT

Supporting Information

The following information is available: (1) Detailed description of the experimental procedures and the statistical analysis methods; (2) Figure S-1 showing PTFE binder plates for our sample holder; (3) Figure S-2 illustrating examples of non-selective Cu plating and patinas due to Pd/Sn release from the paper surface, and; (4) Tables S-1−S-7 summarizing experimental resistance measurements and intermediate calculations associated with the analysis of the factorial design experiments. This material is available free of charge via the Internet at http://pubs.acs.org.

■ AUTHOR INFORMATION

Corresponding Author

*E-mail: walter.dressick@nrl.navy.mil.

Notes

The authors declare no competing financial interest.

■ ACKNOWLEDGMENTS

We gratefully acknowledge financial support for this research from the Office of Naval Research (ONR) through the Naval Research Laboratory Core 6.2 Research Program.

■ REFERENCES

(1) Perelaer, J.; Hendriks, C. E.; de Laat, A. W. M.; Schubert, U. S. *Nanotechnology* **2009**, *20*, No. 165303.
(2) Liu, X.; Chang, H.; Li, Y.; Huck, W. T. S.; Zheng, Z. *ACS Appl. Mater. Interfaces* **2010**, *2*, 529−535.
(3) Schwarz, A.; Hakuzimana, J.; Kaczynska, A.; Banaszczyk, J.; Westbroek, P.; McAdams, E.; Moody, G.; Chronis, Y.; Priniotakis, G.; De Mey, G.; Tseles, D.; Langenhove, L. V. *Surf. Coat. Technol.* **2010**, *204*, 1412−1418.
(4) Siegel, A. C.; Phillips, S. T.; Dickey, M. D.; Lu, N.; Suo, Z.; Whitesides, G. M. *Adv. Funct. Mater.* **2010**, *20*, 28−35.
(5) Wang, C.-W.; Yang, M.-H.; Lee, Y.-Z.; Cheng, K. *J. Imaging Sci. Technol.* **2007**, *51*, 452−455.
(6) Perelaer, J.; Klokkenburg, M.; Hendriks, C. E.; Schubert, U. S. *Adv. Mater.* **2009**, *21*, 4830−4834.
(7) Gan, X.; Wu, Y.; Liu, L.; Shen, B.; Hu, W. *J. Alloys Compd.* **2008**, *455*, 308−313.
(8) Guo, R. H.; Jiang, S. Q.; Yuen, C. W. M.; Ng, M. C. F. *J. Appl. Electrochem.* **2009**, *39*, 907−912.
(9) Guo, T.-F.; Chang, S.-C.; Pyo, S.; Yang, Y. *Langmuir* **2002**, *18*, 8142−8147.
(10) Huang, D.; Liao, F.; Molesa, S.; Redinger, D.; Subramanian, V. *J. Electrochem. Soc.* **2003**, *150*, G412−G417.
(11) Wang, J.-Y.; Huo, S.-J.; Cai, W.-B.; Xu, Q.-J. *Chem. Lett.* **2006**, *35*, 582−583.
(12) Gamerith, S.; Klug, A.; Scheiber, H.; Scherf, U.; Moderegger, E.; List, E. J. W. *Adv. Funct. Mater.* **2007**, *17*, 3111−3118.
(13) Perelaer, J.; de Laat, A. W. M.; Hendriks, C. E.; Schubert, U. S. *J. Mater. Chem.* **2008**, *18*, 3209−3215.
(14) Li, D.; Sutton, D.; Burgess, A.; Graham, D.; Calvert, P. D. *J. Mater. Chem.* **2009**, *19*, 3719−3724.
(15) Sridhar, A.; Reiding, J.; Adelaar, H.; Achterhoek, F.; van Dijk, D. J.; Akkerman, R. *J. Micromech. Microeng.* **2009**, *19*, No. 085020.
(16) Tseng, C.-C.; Chang, C.-P.; Sung, Y.; Chen, Y.-C.; Ger, M.-D. *Coll. Surf. A* **2009**, *339*, 206−210.
(17) Woo, K.; Kim, D.; Kim, J. S.; Lim, S.; Moon, J. *Langmuir* **2009**, *25*, 429−433.
(18) Anto, B. T.; Sivaramakrishnan, S.; Chua, L. L.; Ho, P. K. H. *Adv. Funct. Mater.* **2010**, *20*, 286−303.
(19) Tekin, E.; Smith, P. J.; Schubert, U. S. *Soft Matter* **2008**, *4*, 703−713.
(20) Määttänen, A.; Ihalainen, P.; Pulkkinen, P.; Wang, S.; Tenhu, H.; Peltonen, J. *ACS Appl. Mater. Interfaces* **2012**, *4*, 955−964.
(21) Grouchko, M.; Kamyshny, A.; Magdassi, S. *J. Mater. Chem.* **2009**, *19*, 3057−3062.
(22) Jeong, S.; Woo, K.; Kim, D.; Lim, S.; Kim, J. S.; Shin, H.; Xia, Y.; Moon, J. *Adv. Funct. Mater.* **2008**, *18*, 679−686.
(23) Pulkkinen, P.; Shan, J.; Leppänen, K.; Känsäkoski, A.; Laiho, A.; Järn, M.; Tenhu, H. *ACS Appl. Mater. Interfaces* **2009**, *1*, 519−525.
(24) Magdassi, S.; Grouchko, M.; Berezin, O.; Kamyshny, A. *ACS Nano* **2010**, *4*, 1943−1948.
(25) Tai, Y.-L.; Yang, Z.-G. *J. Mater. Chem.* **2011**, *21*, 5938−5943.
(26) Stamm, A. J. *Wood and Cellulose Science*; The Ronald Press Company: New York, 1964.
(27) Hon, D. N.-S. *Cellulose* **1994**, *1*, 1−24.
(28) Kamide, K.; Saito, M. *Adv. Polym. Sci.* **1987**, *83*, 1−56.
(29) Kobayashi, S.; Uyama, H. *Macromol. Chem. Phys.* **2003**, *204*, 235−256.
(30) Zabetakis, D.; Dressick, W. J. *ACS Appl. Mater. Interfaces* **2009**, *1*, 4−25.
(31) Garcia, A.; Polesel-Maris, J.; Viel, P.; Palacin, S.; Berthelot, T. *Adv. Funct. Mater.* **2011**, *21*, 2096−2102.
(32) Bessueille, F.; Gout, S.; Cotte, S.; Goepfert, Y.; Leonard, D.; Romand, M. *J. Adhes.* **2009**, *85*, 690−710.
(33) Shah, P.; Kevrekidis, Y.; Benziger, J. *Langmuir* **1999**, *15*, 1584−1587.
(34) Zabetakis, D.; Loschialpo, P.; Smith, D.; Dinderman, M. A.; Dressick, W. J. *Langmuir* **2009**, *25*, 1785−1789.
(35) Box, G. E. P.; Hunter, W. G.; Hunter, J. S. *Statistics for Experimenters: An Introduction to Design, Data Analysis, and Model Building*; John Wiley & Sons: New York, 1978.
(36) Dinderman, M. A.; Dressick, W. J.; Kostelansky, C. N.; Price, R. R.; Qadri, S. B.; Schoen, P. E. *Chem. Mater.* **2006**, *18*, 4361−4368.
(37) Chen, M.-S.; Dulcey, C. S.; Brandow, S. L.; Leonard, D. N.; Dressick, W. J.; Calvert, J. M.; Sims, C. W. *J. Electrochem. Soc.* **2000**, *147*, 2607−2610.
(38) Dressick, W. J.; Dulcey, C. S.; Brandow, S. L.; Chen, M.-S.; Leonard, D. N.; Calvert, J. M.; Sims, C. W. In *Electrochemical Technology Applications in Electronics-III (Proceedings of the 1999 Joint International Meeting of the Electrochemical Society)*; Romankiw, L. T., Osaka, T., Yamazaki, Y., Madore, C., Eds.; The Electrochemical Society: Pennington, NJ, 2000; Vol. *99*, p 179−187.
(39) Bindra, P.; White, J. R. In *Electroless Plating-Fundamentals and Applications*; Mallory, G. O., Hajdu, J. B., Eds.; American Electroplaters and Surface Finishers Society: Orlando, FL, 1990, p 289−329.
(40) Zabetakis, D.; Dinderman, M.; Schoen, P. *Adv. Mater.* **2005**, *17*, 734−738.
(41) Souguir, Z.; Dupont, A.-L.; d'Espinose de Lacaillerie, J.-B.; Lavdrine, B.; Cheradame, H. *Biomacromolecules* **2011**, *12*, 2082−2091.
(42) Lamminmäki, T.; Kettle, J.; Rautkoski, H.; Kokko, A.; Gane, P. *Ind. Eng. Chem. Res.* **2011**, *50*, 7251−7263.
(43) Sehaqui, H.; Liu, A.; Zhou, Q.; Berglund, L. A. *Biomacromolecules* **2010**, *11*, 2195−2198.
(44) Griffiths, D. In *Introduction to Electrodynamics*; 3rd ed.; Reeves, A., Ed.; Prentice-Hall: Upper Saddle River, NJ, 1999, p 286.
(45) Dressick, W. J.; Dulcey, C. S.; Georger, J. H.; Calabrese, G. S.; Calvert, J. M. *J. Electrochem. Soc.* **1994**, *141*, 210−220.
(46) Brandow, S. L.; Chen, M.-S.; Wang, T.; Dulcey, C. S.; Calvert, J. M.; Bohland, J. F.; Calabrese, G. S.; Dressick, W. J. *J. Electrochem. Soc.* **1997**, *144*, 3425−3434.
(47) Jacobs, J. W. M.; Rikken, J. M. G. *J. Electrochem. Soc.* **1988**, *135*, 2822−2827.
(48) van der Putten, A. M. T.; de Bakker, J. W. G. *J. Electrochem. Soc.* **1993**, *140*, 2221−2228.
(49) van der Putten, A. M. T.; de Bakker, J. W. G. *J. Electrochem. Soc.* **1993**, *140*, 2229−2235.
(50) Zhang, S.; Debaets, J.; Vereeken, M.; Vervaet, A.; van Claster, A. *J. Electrochem. Soc.* **1999**, *146*, 2870−2875.

(51) O'Sullivan, E. J. In *Electrochemical Technology Applications in Electronics III (Proceedings of the 1999 Joint International Meeting of the Electrochemical Society)*; Romankiw, L. T., Osaka, T., Yamazaki, Y., Madore, C., Eds.; Electrochemical Society: Pennington, NJ, 2000; Vol. *99*, pp 159−171.
(52) Ikeda, A.; Saeki, T.; Sakamoto, A.; Sugimoto, Y.; Kimiya, Y.; Fukunaga, Y.; Hattori, R.; Kuriyaki, H.; Kuroki, Y. *IEEE Trans. Compon. Packag. Technol.* **2007**, *30*, 494−499.
(53) Henriksson, M.; Berglund, L. A.; Isaksson, P.; Lindström, T.; Nishino, T. *Biomacromolecules* **2008**, *9*, 1579−1585.
(54) Nogi, M.; Iwamoto, S.; Nakagaito, A. N.; Yano, H. *Adv. Mater.* **2009**, *21*, 1595−1598.
(55) de Mesquita, J. P.; Donnici, C. L.; Pereira, F. V. *Biomacromolecules* **2010**, *11*, 473−480.
(56) Fernandes, S. C. M.; Freire, C. S. R.; Silvestre, A. J. D.; Neto, C. P.; Gandini, A.; Berglund, L. A.; Salmén, L. *Carbohydr. Polym.* **2010**, *81*, 394−401.
(57) Schmitt, F.; Granet, R.; Sarrazin, C.; Mackenzie, G.; Krausz, P. *Carbohydr. Polym.* **2011**, *86*, 362−366.
(58) Wang, H. F.; Zhang, L. M. *Prog. Chem.* **2010**, *22*, 2165−2172.
(59) Pardal, A. C.; Ramos, S. S.; Santos, L.; Almeida, P. *Color. Technol.* **2001**, *117*, 43−48.
(60) Yang, C. Q.; Wei, W. S.; Lickfield, G. C. *Text. Res. J.* **2000**, *70*, 143−147.
(61) Zhou, Y. J.; Luner, P.; Caluwe, P. *J. Appl. Polym. Sci.* **1995**, *58*, 1523−1534.
(62) Warren, J.; Reid, J. D.; Hamalainen, C. *Text. Res. J.* **1952**, *22*, 584−591.
(63) Welsh, E. R.; Schauer, C. L.; Santos, J. P.; Price, R. R. *Langmuir* **2004**, *20*, 1807−1811.
(64) Obokata, T.; Isogai, A. *Nord. Pulp Paper Res. J.* **2009**, *24*, 135−140.
(65) Xu, G. G.; Yang, C. Q.; Deng, Y. L. *J. Appl. Polym. Sci.* **2004**, *93*, 1673−1680.
(66) Fernandes, S. C. M.; Freire, C. S. R.; Silvestre, A. J. D.; Desbrires, J.; Gandini, A.; Neto, C. P. *Ind. Eng. Chem. Res.* **2010**, *49*, 6432−6438.
(67) Dressick, W. J.; Kondracki, L. M.; Chen, M.-S.; Brandow, S. L.; Matijević, E.; Calvert, J. M. *Colloids Surf. A* **1996**, *108*, 101−111.
(68) Dressick, W. J.; Dulcey, C. S.; Chen, M.-S.; Calvert, J. M. *Thin Solid Films* **1996**, *284*, 568−572.
(69) Chen, M.-S.; Dulcey, C. S.; Chrisey, L. A.; Dressick, W. J. *Adv. Funct. Mater.* **2006**, *16*, 774−783.
(70) Brandow, S. L.; Chen, M.-S.; Fertig, S. J.; Chrisey, L. A.; Dulcey, C. S.; Dressick, W. J. *Chem.—Eur. J.* **2001**, *7*, 4495−4499.
(71) Dressick, W. J.; Chen, M.-S.; Brandow, S. L.; Rhee, K. W.; Shirey, L. M.; Perkins, F. K. *Appl. Phys. Lett.* **2001**, *78*, 676−678.
(72) Dressick, W. J.; Dulcey, C. S.; Brandow, S. L.; Witschi, H.; Neeley, P. F. *J. Vac. Sci. Technol. A* **1999**, *17*, 1432−1440.
(73) Dressick, W. J.; Calvert, J. M. *Jpn. J. Appl. Phys. Part 1* **1993**, *32*, 5829−5839.
(74) Martin, B. D.; Brandow, S. L.; Dressick, W. J.; Schull, T. L. *Langmuir* **2000**, *16*, 9944−9946.
(75) Chen, M.-S.; Brandow, S. L.; Schull, T. L.; Chrisey, D. B.; Dressick, W. J. *Adv. Funct. Mater.* **2005**, *15*, 1364−1375.
(76) Demirel, M. C.; Cetinkaya, M.; Singh, A.; Dressick, W. J. *Adv. Mater.* **2007**, *19*, 4495−4499.
(77) Lee, S. B.; Koepsel, R. R.; Morley, S. W.; Matyjaszewski, K.; Sun, Y.; Russell, A. J. *Biomacromolecules* **2004**, *5*, 877−882.
(78) Suh, S. W.; Lee, Y. S.; Park, B. K.; Kim, D. S. *Jpn. J. Appl. Phys., Part 2* **2010**, No. 05EA06.
(79) Peng, C.; Lo, S. H. Y.; Wan, C.-C.; Wang, Y.-Y. *Colloids Surf., A* **2007**, *308*, 93−99.
(80) Lan, J.-L.; Wan, C.-C.; Wang, Y.-Y. *J. Electrochem. Soc.* **2008**, *155*, K77−K83.
(81) Aldakov, D.; Bonnassieux, Y.; Geffroy, B.; Palacin, S. *ACS Appl. Mater. Interfaces* **2009**, *1*, 584−589.
(82) Li, J.; O'Keefe, M. J.; O'Keefe, T. J. *Surf. Coat. Technol* **2011**, *205*, 3134−3140.
(83) Sawhney, A.; Agrawal, A.; Lo, T.-C.; Patra, P. K.; Chen, C. H.; Calvert, P. *AATCC Rev* **2007**, *7*, 42−46.
(84) Bidoki, S. M.; McGorman, D.; Lewis, D. M.; Clark, M.; Horler, G.; Miles, R. E. *AATCC Rev.* **2005**, *5*, 11−14.
(85) Bidoki, S. M.; Lewis, D. M.; Clark, M.; Vakorov, A.; Millner, P. A.; McGorman, D. *J. Micromech. Microeng* **2007**, *17*, 967−974.